#6189

EVALUATION OF VENTILATION EFFECTIVENESS USING AN IAQ MODEL

Toshiaki Yamamoto and David S. Ensor
Center for Aerosol Technology
Research Triangle Institute
P.O. Box 12194
Research Triangle Park, NC 27709

Leslie E. Sparks
Air and Energy Engineering Research Laboratory
U.S. Environmental Protection Agency
Research Triangle Park, NC 27711

SUMMARY

A new ventilation solver was developed that is capable of determining the distributions of a time-averaged flow field, the effective turbulent diffusion coefficient, and the steady-state or time-dependent contaminant concentration distribution within isothermal indoor space. The model was written for a personal computer and the computational speed is extremely fast (a few minutes) with reasonable accuracy so that engineers can use it as a tool to evaluate ventilation performance in indoor space yet to be built.

Ventilation performance depends on room geometry; ventilation method; operating condition; and location, strength, and types of contaminants. Case studies were performed using a user-friendly indoor air quality (IAQ) model. The ventilation performance was carried out using the proposed new scales called "Ventilation Performance Indices" (VPI1, VPI2, and VPI3): (1) average contaminant concentration or decay rate (VPI1), (2) average contaminant diffusion coefficient (VPI2), and (3) average contaminant concentration or decay rate at the breathing level (VPI3).

EVALUATION OF VENTILATION EFFECTIVENESS USING AN IAQ MODEL

Toshiaki Yamamoto and David S. Ensor
Center for Aerosol Technology
Research Triangle Institute
P.O. Box 12194
Research Triangle Park, NC 27709

Leslie E. Sparks
Air and Energy Engineering Research Laboratory
U.S. Environmental Protection Agency
Research Triangle Park, NC 27711

INTRODUCTION

Indoor air quality is increasingly being recognized as an essential factor for overall health and comfort because people spend a large fraction of their time indoors. Increased awareness of the potential health risks associated with indoor air pollutants has stimulated interest in improving our knowledge about how ventilation air is distributed and transported in indoor space. An effective ventilation tool is needed to help designers choose the optimum design from many possible alternatives.

Most of the numerical models developed to compute airflow distribution and concentration profiles within rooms require either a mainframe or a supercomputer [1-6]. However, these models have limited use because most engineers lack access to mainframes or supercomputers. Even the most complex model contains assumptions affecting the accuracy of the prediction and may not adequately account for the details of room configuration, supply/return air duct location, source location, and inflow velocity.

Our goal was to provide software tools for evaluating the effects of indoor geometry, supply/return duct placement, diffuser design, and operating conditions on ventilation performance that can be used by engineers responsible for indoor air quality. The software was developed for personal computers that now are readily available. By making some compromises with respect to the detail of the computations, it was possible to ensure computational times practical for the capacity of personal computers, while still being able to predict the general behavior of contaminant dispersion in a room, to design

a ventilation system, or to solve sick building problems. For a wide range of practical situations, personal computers have adequate capacity.

The model developed is a two-dimensional k-ε turbulence model that was specifically developed for use on a personal computer. The Navier-Stokes equations and Reynolds stress equations can be expressed in the form of a vorticity-stream function to reduce the governing equations: stream function, vorticity, turbulent kinetic energy, energy dissipation rate, and contaminant diffusion equations. These equations are expressed as a finite difference form and solved simultaneously with appropriate boundary conditions. This model is highly interactive, permitting the user to control the flow of the program. Menus display the choices of the room configurations and operating parameters along with several lines of text on the screen and a flashing cursor [7]. The computational time is very fast (a few minutes) and the results are reasonably accurate. In this model, a mesh point of 25 x 21 (grid size of 6 by 6 in., or 15.24 x 15.24 cm) was used. The detailed computational procedures, and the arguments related to the mesh size for the case of point source in a room, have been described previously [7].

Several concepts to define the ventilation performance already had been discussed at the time this model was developed. Sandberg and Sjoberg [8] introduced the idea of "the age of air" in room, i.e., local-mean age-of-air and room-average age-of-air in order to evaluate ventilation performance. Murakami and Kato [9] discussed Scale of Ventilation Efficiency: SVE1, SVE2, and SVE3. However, no definition of ventilation performance has been fully explored or accepted up to this point. We now propose a new scale called "Ventilation Performance Indices" (VPI1, VPI2, and VPI3); (1) average contaminant concentration or decay rate (VPI1), (2) average contaminant diffusion coefficient (VPI2), and (3) average contaminant concentration or decay rate at the breathing level (VPI3).

Figure 1 shows the room configuration for which the supply (B) and exhaust (T) dimensions, locations (A), room width (W), room height (H), and inflow velocity (U_o) can be specified. For this case study, W=12 ft (3.66 m), H=10 ft (3.05 m), T=2 ft (0.61 m), A=1 ft (0.30 m), 5 ft (1.52 m), 9 ft (2.74 m). For U_o, 10 ft/min (3 m/min) and 50 ft/min (15 m/min) were selected. The first case is where the continuous contaminant generates uniformly throughout the room. The second case is where the room is initially uniformly contaminated and no other source is generated thereafter. The time-dependent concentration decay was computed. The effects of the placement of the supply air duct and inflow velocity on ventilation performance were qualitatively evaluated.

NUMERICAL RESULTS AND DISCUSSION

When a supply duct is placed at the center of the ceiling and an exhaust duct is located at the bottom of the side wall, the time-averaged airflow streamlines in a room are shown in Figure 2. The diagram shows two large recirculation zones with nearly equal strength, one on each side of the main airflow path. The strength of recirculation indicates an

index of how strongly contaminants can be entrained and trapped in the recirculation zone. Flow recirculation clearly is not a favorable condition.

Figure 3 shows the airflow distribution when the supply duct is placed at the left side of the room, while other parameters are unchanged. The airflow distribution is completely modified; one large recirculation is observed at the upper center of the room and one small recirculation is at the left side of the flow entry duct. The air motion in the upper-right section is very small, indicating poor mixing. When the supply air duct is at the right side, the active flow field is shifted right and a large portion of the room is occupied with flow recirculation, as shown in Figure 4. The flow bypass results in poor ventilation. Note that airflow streamlines for a higher flow rate (U_o= 50 ft/min, or 15 m/min) are omitted here but are almost identical.

Most indoor environments are not well mixed but rather are finitely mixed. Therefore, it is important to understand how well the room air is mixed. Because the effective contaminant diffusion coefficients (D_{eff}) represent air mixing, a higher contaminant mixing takes place at the region of higher diffusion. The contaminant diffusion coefficient consists of the diffusion due to Brownian motion and the diffusion due to turbulent kinetic energy. Figures 5, 6, and 7 show the distribution of nondimensionalized D_{eff} when the flow entry is at the center, left, and right, respectively. The actual turbulent diffusion coefficients can be obtained by multiplying U_oB by the values shown in these figures. As shown, the highest diffusion takes place at the flow exit area and the next higher diffusion appears in the vicinities of the inflow and main flow stream region. As distance from the main airflow path increases the contaminant diffusion decreases. General practice is to consider minimizing zones of low contaminant diffusion or poor ventilation. This scale may be used as one measure of ventilation performance (VPI2). For the case of higher inflow velocity (U_o=50 ft/min, or 15 m/min), the distribution of D_{eff} is almost identical to the case for lower velocity but the magnitudes vary with the product of U_o and B.

Figure 8 shows the contours of contaminant concentration that occur when the supply duct is placed at the center of the room. Note that the contaminant level shown here is a relative value. The contaminant concentration is significantly higher on the upper-left and right-hand sides of the room. Placing the supply air duct at the left side of the room creates the contaminant concentration distributions shown in Figure 9. The average contaminant concentration is significantly improved. Shown in Figure 10 is the contaminant distribution when the supply duct is at the right-hand side. The contaminant level for half of the room is very high due to poor mixing. When U_o increases 5 times (50 ft/min, or 15 m/min) for the center entry configuration, the ventilation performance is significantly improved, as shown in Figure 11.

Table 1 summarizes the average contaminant concentration in the room (C_{ave}), average contaminant at the breathing level between 3.5 ft (1.05 m) and 6.0 ft (1.8 m) from the floor (C_{aveb}), maximum contaminant level (C_{max}), fraction of the contaminant level not to exceed 5% of C_{ave} (C5), fraction of the contaminant level not to exceed 10% of C_{ave} (C10), fraction of the contaminant level not to exceed 50% of C_{ave} (C50), average

contaminant diffusion coefficient (D_{eff}) in m^2/s, and maximum and minimum stream function (P_{max}, P_{min}).

Because C_{aveb} depends on the ventilation parameters discussed and may be different from the average contaminant, it takes into account into the ventilation performance (VPI3) as well as C_{ave} (VPI1) and D_{eff} (VPI2). Note that C_{aveb} is always lower than C_{ave}. The best ventilation performance obtained is the right flow entry case for a given air exchange rate.

The ventilation performance can be defined as the ratio of either C_{ave} with flow/C_{ave} without flow or $C(\tau)/C(t=0)$, and it can be argued using either the constant steady source case discussed in the first half of this paper or the time-dependent concentration case discussed in the latter half.

Table 1. Summary of C_{ave}, C_{aveb}, C_{max}, C5, C10, C50, D_{eff}, P_{max}, P_{min}.

	Center Entry U_o=10 ft/min (3 m/min)	Left Entry U_o=10 ft/min	Right Entry U_o=10 ft/min	Center Entry U_o=50 ft/min (15 m/min)
C_{ave}	1.333	0.964	2.824	0.268
C_{aveb}	1.296	0.917	2.446	0.260
C_{max}	2.61	2.51	5.31	0.528
C5	0.027	0.112	0.140	0.030
C10	0.064	0.197	0.181	0.066
C50	0.435	0.652	0.373	0.435
D_{eff}	0.0095	0.0144	0.0080	0.0095
P_{max}	1.12	1.11	1.04	1.12
P_{min}	-0.11	-0.04	-0.14	-0.11

The next case is one in which the room is initially contaminated (no further contaminants are generated thereafter), while a steady-state flow field exists, and the time-dependent contaminant distribution is computed as a function of the nondimensionalized time scale t=10, 30, 60. A time t=30 corresponds to the characteristic time (τ). Note that the actual time is obtained by multiplying B/U_o.

Figures 12(a)-(c) show the contaminant concentration decay as a function of time when the supply duct is at the center. The values of C_{ave}, C_{aveb}, and C_{max} are recorded. The

average concentration decays exponentially because of finite mixing. Figures 13(a)-(c) show the time-dependent contaminant concentration when the supply duct is at the left. The average concentration is considerably improved in comparison with the center entry case. Figures 14(a)-(c) show the time-dependent contaminant concentration when the supply duct is placed at the right. The average concentration is the worst among the three cases because a large fraction of the room is unmixed due to flow bypass. As the time elapses, an extremely high concentration is observed at the upper-right corner of the room where the recirculation exists. Apparently, the ventilation performance improves with increased U_o. In order to increase the ventilation performance, the value of D_{eff} must be increased by increasing the gas passage length in the room. The higher D_{eff}, the better the ventilation performance. The finitely mixed case shows always less ventilation performance than a well mixed case.

CONCLUSIONS

A user-friendly ventilation model was developed to provide an analytical tool for engineers who need to evaluate indoor air quality engineering problems. The model operates on a personal computer with appropriate accuracy and resolution, and provides rapid analysis of airflow and contaminant concentration distributions.

Ventilation effectiveness depends on room configuration; ventilation methods; operating conditions; and location, strength, and types of contaminants. New scales called "Ventilation Performance Indices" (VPI1, VPI2, and VPI3) are proposed to evaluate the ventilation effectiveness: (1) average contaminant concentration or decay rate of the room (VPI1), (2) average contaminant diffusion coefficient (VPI2), and (3) average contaminant concentration and decay rate at the breathing level (VPI3).

REFERENCES

[1] Kurabuchi, T., Sakamoto, Y., and Kaizuka, M. "**Numerical Prediction of Indoor Airflows by Means of the k-ε Turbulence Model**". Proceedings of Building Systems: Room Air and Air Contaminant Distribution, ASHRAE, 1989, pp. 57-67.

[2] Murakami, S. and Kato, S. "**Current Status of Numerical and Experimental Methods for Analyzing Flow Field and Diffusion Field in a Room**". Proceedings of Building Systems: Room Air and Air Contaminant Distribution, ASHRAE, 1989, pp. 39-56.

[3] Baker, A.J. and Kelso, R.M. "**On Validation of Computational Fluid Dynamics Procedures for Room Air Motion Prediction**". ASHRAE Trans., 1990, Vol. 96, pp. 760-774.

[4] Kelso, R.M., Wilkening, L.E., Schaub, E.G. and Baker, A.J. "**Computational Simulation of Kitchen Airflows with Commercial Hoods**". In Proceedings of 1992 ASHRAE Winter Meeting, 1992, 3565.

[5] Chen, Q., and Jiang, Z. "**Significant Questions in Predicting Room Air Motion**". In Proceedings of 1992 ASHRAE Winter Meeting, AN-92-9-1, 1992.

[6] Kuehn, T.H., Pui, D.Y.H., and Gratzek J.P. "**Experimental and Numerical Results for Airflow and Particle Transport in a Microelectronics Clean Room**". In Proceedings of 1992 ASHRAE Winter Meeting, AN-92-9-2, 1992.

[7] Yamamoto, T., Ensor, D.S., and Sparks, L.E. "**Two-Dimensional Turbulence Model for a Personal Computer**". In Proceedings of IAQ'91 Healthy Buildings, Washington, DC, Sept. 4-8, 1991, pp. 175-178.

[8] Sandberg, M., M. Sjoberg, "**The Use of Moments for Assessing Air Quality in Ventilated Room**". Building and Environment, Vol. 18, No. 4, 1983, pp. 181-197.

[9] Murakami, S. and Kato, S. "**Flow and Diffusion Field in a Clean Room**". Journal of Aerosol Research, Japan, Vol. 3, No. 4, 1988, pp. 262-272.

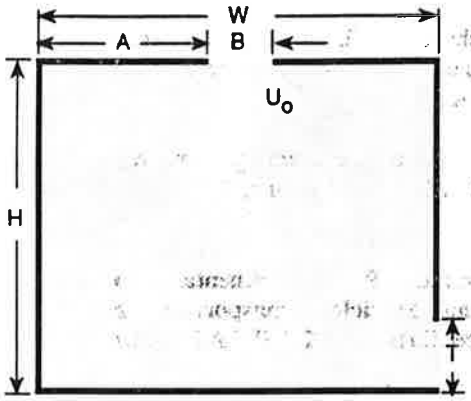

Figure 1. Room outline and variables.

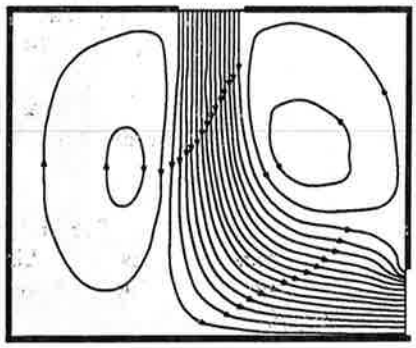

Figure 2. Time-averaged airflow streamlines for the center entry.

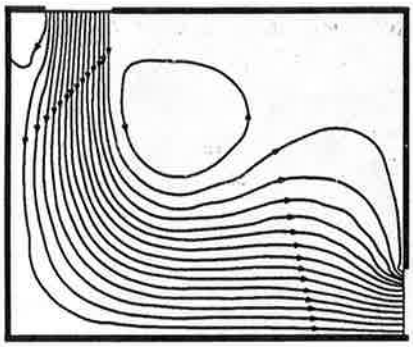

Figure 3. Time-averaged airflow streamlines for the left entry.

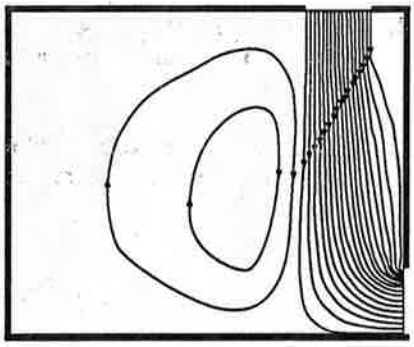

Figure 4. Time-averaged airflow streamlines for the right entry.

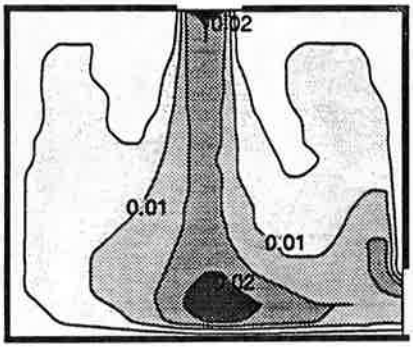

Figure 5. Distribution of D_{eff} for the center entry.

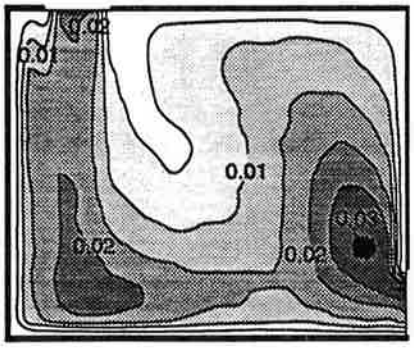

Figure 6. Distribution of D_{eff} for the left entry.

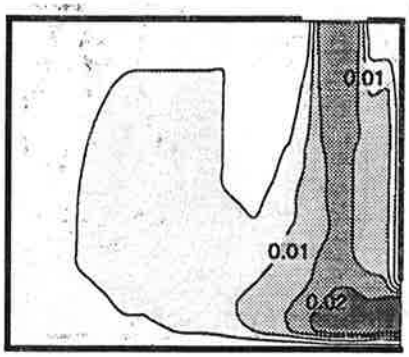

Figure 7. Distribution of D_{eff} for right entry.

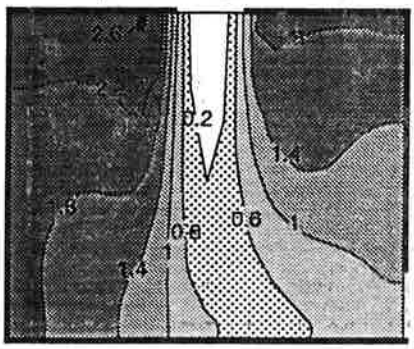

Figure 8. Contours of contaminant distribution for the center entry.

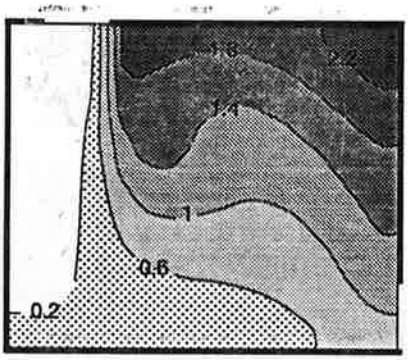

Figure 9. Contours of contaminant distribution for the left entry.

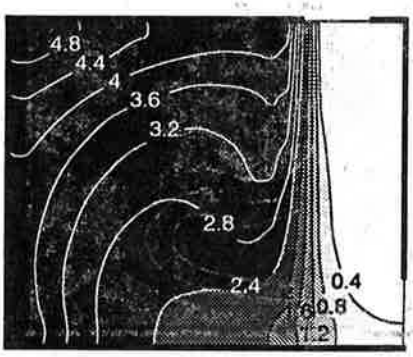

Figure 10. Contours of contaminant distribution for the right entry.

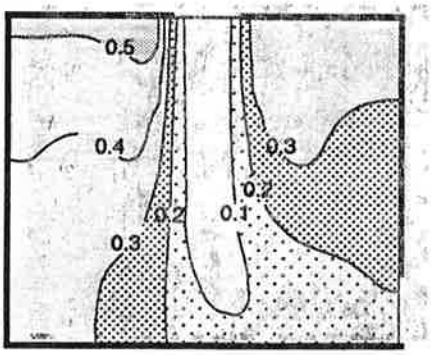

Figure 11. Contours of contaminant distribution for the center entry with high velocity.

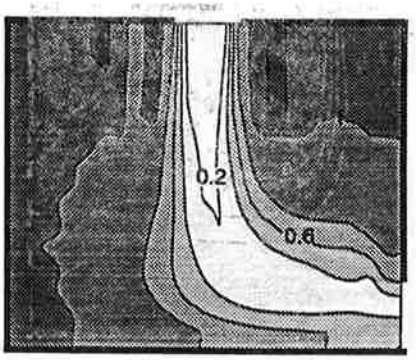

Figure 12a. Contaminant concentration for the center entry at t=10.

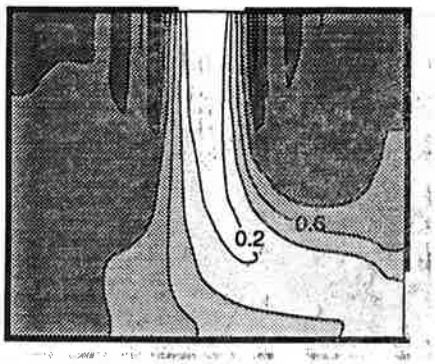

Figure 12b. Contaminant concentration for the center entry at t=30.

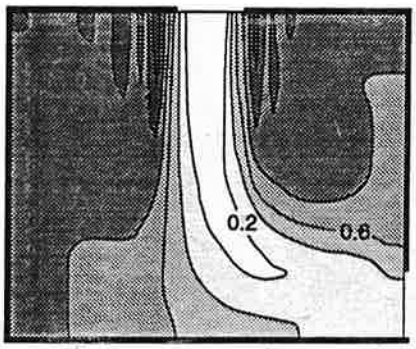

Figure 12c. Contaminant concentration for the center entry at t=50.

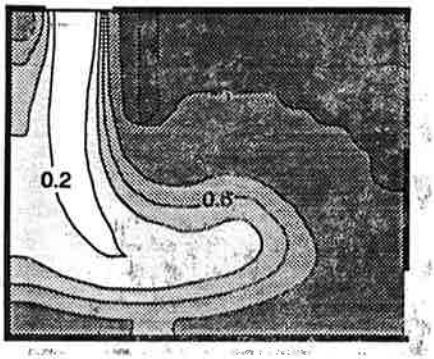

Figure 13a. Contaminant concentration for the left entry at t=10.

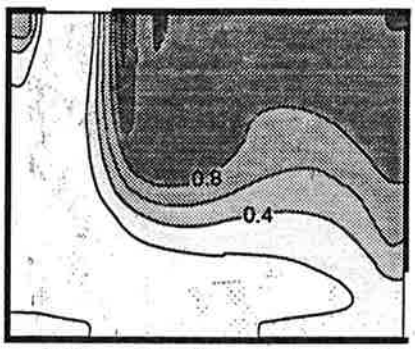

Figure 13b. Contaminant concentration for the left entry at t=30.

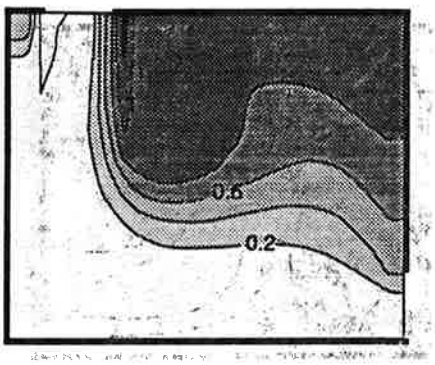

Figure 13c. Contaminant concentration for the left entry at t=50.

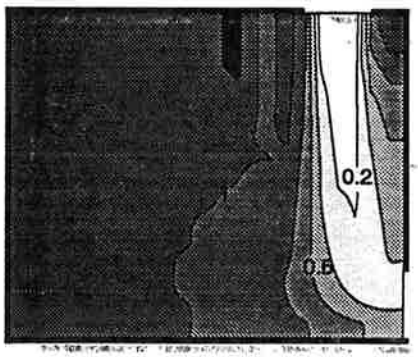

Figure 14a. Contaminant concentration for the right entry at t=10.

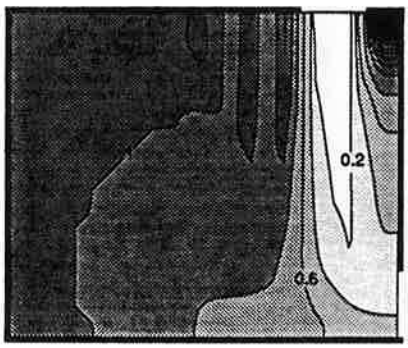

Figure 14b. Contaminant concentration for the right entry at t=30.

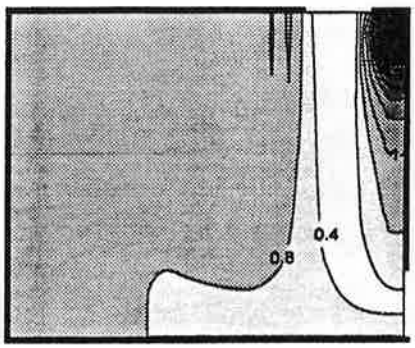

Figure 14c. Contaminant concentration for the right entry at t=50.